

# Solubility of CO<sub>2</sub> in Ionic Liquids with Additional Water and Methanol: Modeling with PC-SAFT Equation of State

Xinyu Liao, Ke Zheng,\* Gang Wang, Yong Yang, Yongwang Li, and Marc-Olivier Coppens\*

Cite This: <https://doi.org/10.1021/acs.iecr.2c02778>

Read Online

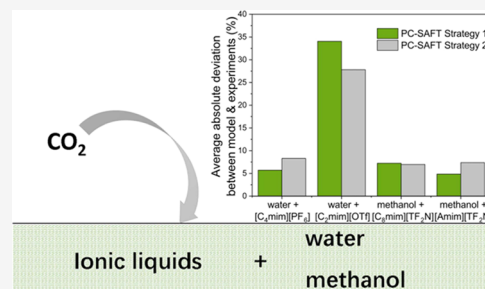
ACCESS |

Metrics & More

Article Recommendations

Supporting Information

**ABSTRACT:** The superior properties of specific ionic liquids (ILs), such as negligible volatility, high thermal stability, flexible designability, and their affinity to capture CO<sub>2</sub>, make them an attractive alternative to chemical and physical solvents that are currently used in CO<sub>2</sub> capture processes. However, a limitation to use ILs for industrial CO<sub>2</sub> capture is their high viscosity compared to conventional solvents, which leads to a lower CO<sub>2</sub> capture rate and higher pumping cost. The viscosity of ILs can be reduced by adding a co-solvent, such as water or methanol. In this work, solubility, vapor–liquid equilibria (VLE), and liquid–liquid equilibria (LLE) for binary and ternary mixtures involving CO<sub>2</sub>, ILs, water, and methanol have been systematically investigated by employing perturbed-chain statistical associating fluid theory (PC-SAFT) equation of state with two different strategies. ILs were considered as self-associating chain molecules with two association sites in the first strategy. As a comparison, they were regarded as strong electrolytes that dissociate into anions and cations in the second strategy. It was found that both strategies provide accurate correlations in modeling CO<sub>2</sub> solubilities in ILs and LLE of binary ILs/water systems. Four ternary systems were selected to verify the predictive capability of the two strategies. For water-containing systems, both strategies performed excellently when binary interaction parameters (BIPs) can be obtained by fitting to experimental data, while they performed poorly for system with few experimental data. For cases where methanol acted as a co-solvent, accurate predictions were obtained with both strategies, even without any BIPs. PC-SAFT was found to be a potential practical tool to develop CO<sub>2</sub> capture processes with new alternative solvents when there are sufficient experimental data for binary mixtures.



## 1. INTRODUCTION

Increasing concerns of global warming resulting from greenhouse gas emissions have stimulated the development of advanced technologies to mitigate carbon dioxide (CO<sub>2</sub>) emissions.<sup>1,2</sup> Carbon capture and storage (CCS), which emphasizes the development of CO<sub>2</sub> capture methods and sequestration technologies, are primarily used to reduce CO<sub>2</sub> emissions from the use of fossil fuels. CCS involve CO<sub>2</sub> separation, capture, transportation, and storage in which CO<sub>2</sub> separation and capture are the most important step.<sup>3</sup>

The technologies for capture and separation of CO<sub>2</sub> include absorption, adsorption, membrane filtration, cryogenic separation, and microbial-based processes.<sup>4</sup> Among these technologies, absorption is the most commonly employed technology for CO<sub>2</sub> capture in large-scale applications. According to the type of solvent, absorption processes can be divided into two subcategories, including chemical absorption and physical absorption. Aqueous amines, due to their higher purification of the gases and a higher CO<sub>2</sub> absorption capacity, are widely used as the absorbent in carbon capture operations and commercialized for many decades.<sup>4–6</sup> Though there are many advantages, the inherent properties of amines also lead to some drawbacks, including low CO<sub>2</sub> loading capacity, high corrosion rate, high regeneration cost, and large equipment size.<sup>5</sup> The physical absorption process is superior to chemical absorption

when the concentration of CO<sub>2</sub> is high due to their low regeneration cost and product loss.<sup>3,7,8</sup> However, due to the high vapor pressure and high volatility of the physical solvent, specifically for the Rectisol process with methanol as a solvent, the absorption process must be operated at a low temperature and high pressure to avoid significant solvent loss.<sup>9,10</sup>

To be more cost-effective for large-scale industrial applications, much research has been devoted to finding or designing new solvents for CO<sub>2</sub> capture. Ionic liquids (ILs) have gained a lot of attention as potential alternatives to replace amine-based chemical absorbents and conventional physical absorbents in CO<sub>2</sub> absorption.<sup>11–15</sup> The exceptional physical and chemical properties, including high CO<sub>2</sub> solubility, high thermal stability, non-flammability, negligible volatility, tunability, and recyclability make ILs ideal solvents in CO<sub>2</sub> capture processes, because they are environmentally friendlier and cheaper for solvent regeneration. Furthermore, the tunability of ILs provides an

Received: August 2, 2022

Revised: September 6, 2022

Accepted: September 7, 2022

Table 1. Pure Parameters for CO<sub>2</sub>, Water, and Methanol

	$M_w$ (g/mol)	$m$	$\sigma$ (Å)	$u/k$ (K)	$\epsilon^{A,B}$ (K)	$\kappa^{A,B}$	refs
CO <sub>2</sub>	44.010	2.0729	2.7852	169.21			45
water	18.015	1.6619	2.4643	267.71	2500.57	0.12502	49
methanol	32.042	1.8458	3.0530	193.94	2668.26	0.04647	49

Table 2. Pure Parameters for ILs in Strategy 1

	$M_w$ (g/mol)	$m$	$\sigma$ (Å)	$u/k$ (K)	$\epsilon^{A,B}$ (K)	$\kappa^{A,B}$	refs
[C <sub>4</sub> mim][PF <sub>6</sub> ]	284.00	2.2820	5.2010	456.29	3450.0	0.00225	43
[C <sub>2</sub> mim][OTf]	260.23	6.3641	3.5543	329.40	4350.6	0.09298	35
[C <sub>2</sub> mim][TF <sub>2</sub> N]	391.32	8.6940	3.5800	378.00	1350.0	0.00225	36
[C <sub>4</sub> mim][TF <sub>2</sub> N]	419.36	9.2600	3.6600	383.00	1350.0	0.00225	36
[C <sub>6</sub> mim][TF <sub>2</sub> N]	447.00	10.100	3.7000	383.00	1350.0	0.00225	36
[C <sub>8</sub> mim][TF <sub>2</sub> N]	475.48	10.400	3.7900	385.00	1350.0	0.00225	36
[Amim][TF <sub>2</sub> N]	403.30	5.7629	4.1600	368.49	3450.0	0.00225	this work

extra degree of freedom for specific modifications to improve the CO<sub>2</sub> capacity and selectivity.<sup>14</sup> On the other hand, the much higher viscosity of ILs than those of conventional solvents is one of the main limitations of their industrial application due to higher pumping and related operating costs. Furthermore, the high viscosity of ILs will significantly inhibit the mass transfer of CO<sub>2</sub> in ILs, resulting in a low absorption rate.<sup>16</sup> To reduce the viscosity of ILs, a third solvent can be introduced as a co-solvent. Water and several organic solvents were found to reduce the viscosity of pure ILs sharply by adding them in small amounts as co-solvents.<sup>17–22</sup>

The measurement and simulation of CO<sub>2</sub> solubility in pure ILs were systematically investigated by an enormous amount of research studies.<sup>23–30</sup> The perturbed-chain statistical associating fluid theory (PC-SAFT) equation of state (EoS) derived using Wertheim's first-order thermodynamic perturbation theory<sup>31–34</sup> was recommended to model IL-containing systems due to their physical background.<sup>23,28,35–37</sup> Baramaki et al. employed PC-SAFT to model CO<sub>2</sub> solubilities in 16 ILs using a temperature-independent interaction parameter, and excellent results were obtained.<sup>35</sup> Solubility of acid gases (CO<sub>2</sub> and H<sub>2</sub>S) in [C<sub>*n*</sub>mim][NTf<sub>2</sub>] (where *n* = 2, 4, 6, and 8) ILs was modeled by Al-finaish and Lue with PC-SAFT using two strategies and four different self-association schemes.<sup>36</sup> They found that the four-site association scheme provided the best results for almost all of the investigated acid gases–IL binary systems and successfully represented solubility of CO<sub>2</sub> and H<sub>2</sub>S in [C<sub>8</sub>mim]-[NTf<sub>2</sub>]. Bülow et al. incorporated a concentration-dependent dielectric constant into electrolyte PC-SAFT to model liquid–liquid equilibria of binary mixtures containing water and commonly used hydrophobic ILs.<sup>37</sup> This new approach was superior, with better correlation capability, compared to the original model whose dielectric constant was independent with concentration. Compared to popular studies on pure ILs, the effects of water and methanol as co-solvents on the solubility of CO<sub>2</sub> in ILs have been experimentally measured and theoretically modeled only by few researchers.<sup>38–44</sup> Valuable experimental data and suitable thermodynamic models for selected systems can be obtained from these works; however, there is no thermodynamic model as yet that can predict the solubility of CO<sub>2</sub> in mixtures of ILs and co-solvents using only binary data for CO<sub>2</sub>/ILs, CO<sub>2</sub>/co-solvents, and ILs/co-solvents, which are more easily measured than data for ternary systems. The goal of this work is to develop a reliable thermodynamic model based on PC-SAFT that can predict the solubility of CO<sub>2</sub> in multi-

component solvents containing ILs and water or methanol from a single set of binary interaction parameters only fitted to binary phase equilibria data. Due to the limitations of available experimental data for ternary mixtures and their binary subsystems, the ILs under investigation contain only few common IL cations of [C<sub>*n*</sub>mim]<sup>+</sup> (where *n* = 2, 4, 6, and 8) and [Amim]<sup>+</sup> and IL anions of [PF<sub>6</sub>]<sup>−</sup>, [OTf]<sup>−</sup>, and [TF<sub>2</sub>N]<sup>−</sup>. However, this is enough to validate the model.

## 2. THEORY

**2.1. PC-SAFT and Modeling Strategies.** The original PC-SAFT EoS developed by Gross and Sadowski<sup>45,46</sup> and its extended version to electrolytes, referred to as electrolyte PC-SAFT (ePC-SAFT),<sup>37,47,48</sup> were used to model thermodynamic properties for systems containing ILs. The expression of the model in terms of the residual Helmholtz free energy  $a^{\text{res}}$  is as follows

$$a^{\text{res}} = a^{\text{hc}} + a^{\text{disp}} + a^{\text{assoc}} + a^{\text{ion}} \quad (1)$$

where  $a^{\text{hc}}$  is the reference hard-chain contribution,  $a^{\text{disp}}$  denotes the dispersion contribution,  $a^{\text{assoc}}$  represents the association contribution referring to site–site association interactions, and  $a^{\text{ion}}$  represents the electrolyte contribution caused by ion–ion interactions. Three pure-component parameters are used in PC-SAFT for non-associating components, including segment number ( $m$ ), segment diameter ( $\sigma$ ), and dispersion energy ( $u/k$ ). Two more associating parameters, association energy  $\epsilon^{A,B}$ , and association volume  $\kappa^{A,B}$ , are introduced to describe hydrogen-bonding interactions between associating molecules. For mixtures, Berthelot–Lorentz combining rules are used

$$u_{ij} = \sqrt{u_i u_j} (1 - k_{ij}) \quad (2)$$

$$\sigma_{ij} = \frac{1}{2} (\sigma_i + \sigma_j) (1 - l_{ij}) \quad (3)$$

where  $k_{ij}$  and  $l_{ij}$  are binary interaction parameters (BIPs) to correct interactions of unlike molecules. An asymmetric BIP,  $p_{ij}$ , which had shown significant improvement to model correlations and predictions in previous works,<sup>49,50</sup> was also introduced in this work.

Besides,  $k_{ij}$  is defined as a temperature-dependent parameter

$$k_{ij} = a_0 + \frac{a_1 T}{1000} \quad (4)$$

where  $a_i$  are constants and  $T$  is the temperature in kelvin.

Pure-component parameters for CO<sub>2</sub>, water, and methanol are given in Table 1. The two-site association scheme was employed to water and methanol. In this work, two strategies were adopted to model ILs. In the first strategy (i.e., original PC-SAFT, strategy 1), ILs were also considered as self-associating chain molecules with two association sites, and the association interaction was allowed between two different sites of two IL molecules or an IL with another association molecule. Pure-component parameters for ILs used in this work are summarized in Table 2. Parameters for [Amim][TF<sub>2</sub>N] were regressed by fitting to liquid density data<sup>51</sup> with 0.14% absolute average deviation (AAD) between theoretical and experimental values. The cross-association parameters can be determined from pure-component association parameters using combining rules

$$\varepsilon^{A,B_j} = \frac{1}{2}(\varepsilon^{A,B_i} + \varepsilon^{A,B_j}) \quad (5)$$

$$\kappa^{A,B_j} = \sqrt{\kappa^{A,B_i} \kappa^{A,B_j}} \left( \frac{2\sqrt{\sigma_{ii}\sigma_{jj}}}{\sigma_{ii} + \sigma_{jj}} \right)^3 \quad (6)$$

In contrast, in the second strategy (i.e., ePC-SAFT, strategy 2), the ILs were treated as strong electrolytes that completely dissociate into cations and anions. IL ions were characterized by three adjustable pure-component parameters ( $m$ ,  $\sigma$ ,  $u/k$ ) and their electric charge with parameter values summarized in Table 3. The AAD for [Amim][TF<sub>2</sub>N] is 0.17% in this strategy. A

Table 3. Pure Parameters for IL Ions in Strategy 2

	$M_w$ (g/mol)	$m$	$\sigma$ (Å)	$u/k$ (K)	refs
[C <sub>2</sub> mim] <sup>+</sup>	111.168	1.4872	3.5926	206.4924	37
[C <sub>4</sub> mim] <sup>+</sup>	139.221	2.4805	3.6371	218.1441	37
[C <sub>6</sub> mim] <sup>+</sup>	167.275	3.4131	3.6781	230.0000	37
[C <sub>8</sub> mim] <sup>+</sup>	195.328	4.2977	3.7187	242.0000	37
[Amim] <sup>+</sup>	123.155	1.7970	3.6245	226.9787	this work
[PF <sub>6</sub> ] <sup>-</sup>	144.973	4.2771	3.5889	492.2835	37
[OTf] <sup>-</sup>	149.070	3.7432	3.8771	509.3113	37
[TF <sub>2</sub> N] <sup>-</sup>	280.145	6.0103	3.7469	375.6529	37

concentration-dependent dielectric constant  $\varepsilon(x)$  was introduced to account for the influence of concentration on the dielectric constant in mixtures

$$\varepsilon = \sum_i^n \varepsilon_i x_i \quad (7)$$

The corresponding  $a^{\text{ion}}$  is shown as follows

$$a^{\text{ion}} = -\frac{\kappa(\varepsilon(x))}{12\pi k_B T \varepsilon(x)} \sum_j q_j^2 x_j \chi_j(\varepsilon(x)) \quad (8)$$

where  $x_i$  and  $q_i$  are the mole fraction and the charge for ion  $i$ , respectively. The Debye screening length  $\kappa$  and the quantity  $\chi_i$  are expressed by

$$\kappa = \sqrt{\frac{\rho_N}{k_B T \varepsilon(x)} \sum_i q_i^2 x_i \varepsilon(x)} \quad (9)$$

$$\chi_i = \frac{3}{(\kappa(\varepsilon(x))\sigma_i)^3} \left[ \frac{3}{2} + \ln(1 + \kappa(\varepsilon(x))\sigma_i) - 2(\kappa(\varepsilon(x))\sigma_i) + \frac{1}{2}(\kappa(\varepsilon(x))\sigma_i)^2 \right] \quad (10)$$

Here,  $\rho_N$  is the number density of the system.

The derivative of the dielectric constant with respect to mole fraction, which is needed in the calculations of the chemical potential, is simplified to

$$\frac{d\varepsilon}{dx_i} = \varepsilon_0 \varepsilon_{r,i} \quad (11)$$

where  $\varepsilon_0$  is the permittivity in vacuo and  $\varepsilon_{r,i}$  is the relative permittivity of the pure component. The relative permittivity for the investigated ILs was set to 11, according to Bülow et al.,<sup>37</sup> those for water and methanol were obtained from the literature, as shown in eqs 12 and 13,<sup>52,53</sup> and for CO<sub>2</sub>, it was set to unity.

$$\varepsilon_{r,\text{water}} = 7.655618295 \times 10^{-4} T^2 - 0.81783881423 T + 254.19616803 \quad (12)$$

$$\varepsilon_{r,\text{methanol}} = -53.398 \ln(T) + 336.170 \quad (13)$$

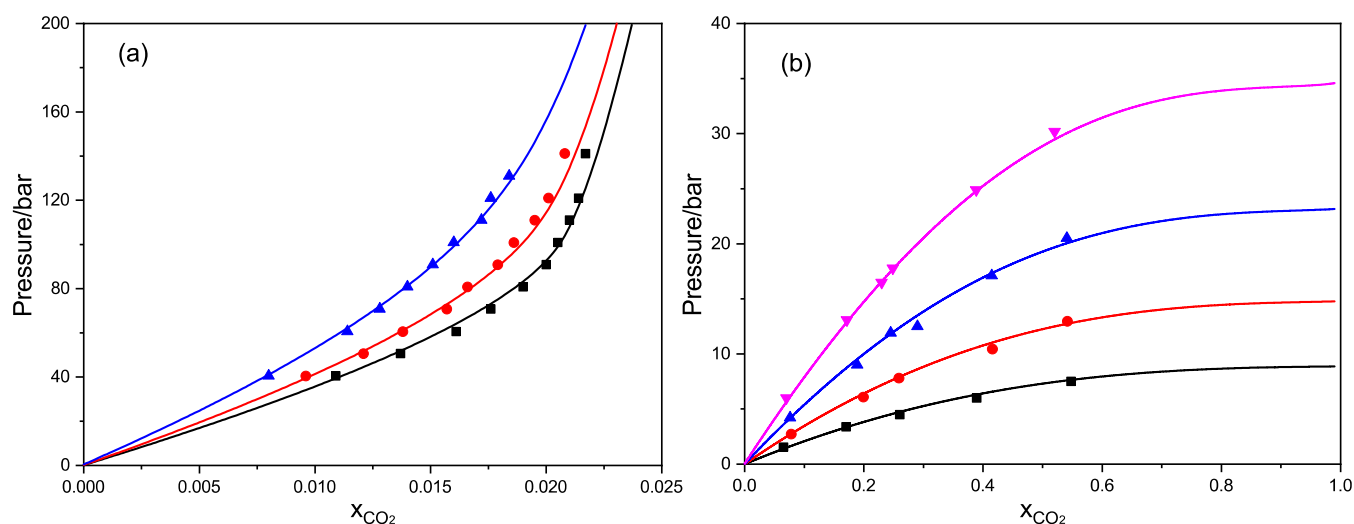


Figure 1. Solubilities of CO<sub>2</sub> in (a) water (black for 323.2 K, red for 333.2 K, and blue for 353.1 K) and (b) methanol (black for 228.2 K, red for 243.2 K, blue for 258.2 K, and magenta for 273.2 K). Comparisons of PC-SAFT (lines) to experimental data<sup>40,54</sup> (symbols).

**2.2. Phase Equilibria.** To calculate the solubility of CO<sub>2</sub> in water or methanol, equality of the fugacity for each component in the liquid and vapor phase should be achieved

$$x_i \hat{\phi}_i^L(T, P, x_i) = y_i \hat{\phi}_i^V(T, P, y_i) \quad (14)$$

where  $\hat{\phi}_i^V$  and  $\hat{\phi}_i^L$  refer to the fugacity coefficients of component  $i$  in either vapor or liquid phase and  $x_i$  and  $y_i$  are mole fractions of component  $i$  in liquid and vapor phases, respectively.

As ILs are nearly nonvolatile, eq 14 for vapor–liquid equilibria (VLE) involving ILs can be reduced to

$$x_i \hat{\phi}_i^L(T, P, x_i) = \hat{\phi}_i^V(T, P) \quad (15)$$

( $i$  is a component other than IL)

For the calculation of liquid–liquid equilibria (LLE) for binary mixtures of water and IL, the phase equilibrium equations become

$$x_i^{L1} \hat{\phi}_i^{L1}(T, P, x_i^{L1}) = x_i^{L2} \hat{\phi}_i^{L2}(T, P, x_i^{L2}) \quad (16)$$

where  $\hat{\phi}_i^{L1}$  and  $\hat{\phi}_i^{L2}$  denote the fugacity coefficients of ILs or water in liquid phases 1 and 2.  $x_i^{L1}$  and  $x_i^{L2}$  are the mole fractions of component  $i$  in each liquid phase.

### 3. RESULTS AND DISCUSSION

The predictive capability is the most significant measure for the quality of a thermodynamic model. In this work, several ternary systems containing CO<sub>2</sub>, ILs, and two important co-solvents (i.e., water and methanol) were selected to validate the predictive capability of PC-SAFT in IL-containing systems. BIPs were acquired by only fitting to binary VLE data or LLE data, and experimental data for ternary mixtures were never used for parameter estimation. The regressions were performed by the least-square method with the residuals defined as the difference between the calculated and experimental values of the CO<sub>2</sub> solubility. The values of the BIPs for the systems investigated are summarized in Tables S1–S5 in the Supporting Information.

**3.1. Solubility of CO<sub>2</sub> in Pure Solvents.** First, solubilities of CO<sub>2</sub> in water and methanol were calculated with PC-SAFT. The  $P - x$  phase diagrams in Figure 1 illustrate that the calculations are in good agreement with the experimental values. The estimated BIPs and AAD (%) are represented in Table S1 in the Supporting Information.

The solubilities of CO<sub>2</sub> in ILs including [C<sub>4</sub>mim][PF<sub>6</sub>], [C<sub>2</sub>mim][OTf], [C<sub>*n*</sub>mim][TF<sub>2</sub>N], and [Amim][TF<sub>2</sub>N] were modeled using two strategies. For strategy 1, the BIPs between CO<sub>2</sub> and ILs were obtained by simply fitting to the corresponding experimental solubility data for each pair. For strategy 2, the BIPs between CO<sub>2</sub> and IL cations or IL anions were the same for all ILs composed of these IL ions. Thus, the values of BIPs in strategy 2 were simultaneously obtained by fitting all of the experimental data together. The comparisons between results calculated using the two strategies are summarized in Figure 2. More details are listed in Tables S2 and S3. As can be observed in Figure 2, the theoretical calculations from both strategies exhibit excellent accuracy in calculations of CO<sub>2</sub> solubilities in ILs. The average AAD (%) for these two strategies are 4.35 and 2.75%, respectively. As a whole, strategy 2 is superior to strategy 1 for the selected cases except, perhaps, for the [C<sub>4</sub>mim][PF<sub>6</sub>]-containing system, where the difference is insignificant. Figure 3 represents typical  $P - x$  phase

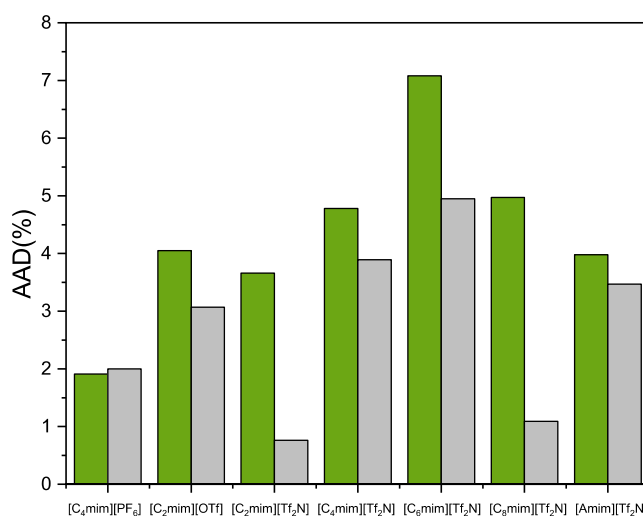


**Figure 2.** AAD (%) between calculated and experimental CO<sub>2</sub> solubilities in ILs using two calculation strategies: green for strategy 1 (fitted for ion pairs) and gray for strategy 2 (joint fits with ion-based parameters).

diagrams for the CO<sub>2</sub> solubility in ILs. It can be observed that strategy 2 performs better than strategy 1 in the range of high pressures, which are close to the critical region of CO<sub>2</sub>. These results indicate that an ion-based model is more suitable to model CO<sub>2</sub> solubility in ILs, especially at high pressure.

**3.2. Mutual Solubility of Water and ILs.** Mutual solubilities of water and ILs, including [C<sub>*n*</sub>mim][TF<sub>2</sub>N], [C<sub>4</sub>mim][PF<sub>6</sub>], and [C<sub>8</sub>mim][OTf], were investigated. The AADs, along with BIPs used in both strategies, are depicted in Figure 4 and are listed in Tables S4 and S5, respectively. The BIPs were obtained with the same approach as for CO<sub>2</sub> and ILs. Collectively, correlations of both strategies match experimental values very well in all selected cases, with an average AAD below 5% for the solubility of water in ILs and the solubility of ILs in water. However, it is hard to distinguish which strategy is best, because both strategies show smaller deviations in some cases and larger ones in other cases. Typical results for mutual solubilities of water and [TF<sub>2</sub>N]<sup>−</sup>-based imidazolium ILs (with [C<sub>*n*</sub>mim]<sup>+</sup> as cations) are presented in Figure 5. Both water solubilities in the IL-rich phase and IL solubilities in the water-rich phase increase with temperature and decrease monotonically with the growth of the alkyl chain length ( $n$ ) of [C<sub>*n*</sub>mim]<sup>+</sup>; the solubilities of ILs in water decrease orders of magnitude as  $n$  increases, as shown in Figure 5b. Obviously, both strategy 1 and strategy 2 provide accurate correlation results in all cases, especially for the solubilities of ILs in water.

**3.3. Solubility of CO<sub>2</sub> in Mixtures of ILs and Co-solvents.** The ultimate goal of this work is to develop a thermodynamic model that can predict CO<sub>2</sub> solubility in multicomponent fluids containing ILs and co-solvents. Experimental data of binary mixtures are ideal for parameter estimation of the model, while the ternary experimental data present an excellent opportunity to test its predictive capability. Thus, VLE of four ternary systems, including CO<sub>2</sub>, ILs, and water or methanol, were predicted with the two described strategies. It should be emphasized that all parameters in this section were obtained by fitting to binary data and that ternary data were never used for parameter estimation. The detailed validation results are summarized in Figure 6 and Table S6. BIPs for [C<sub>2</sub>mim][OTf] and water in strategy 1 were set equal to 0;



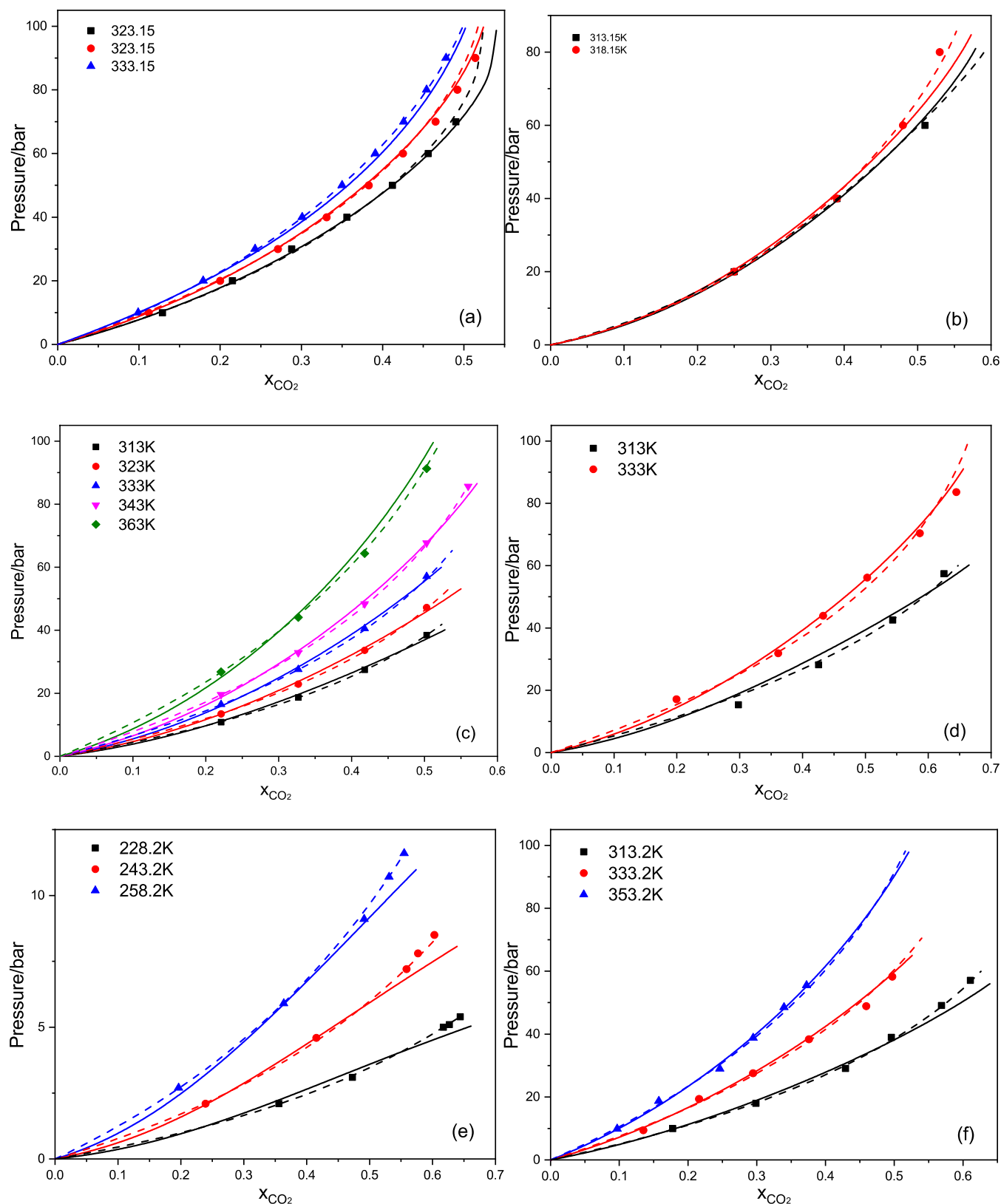


**Figure 3.** Solubilities of CO<sub>2</sub> in (a) [C<sub>4</sub>mim][PF<sub>6</sub>], (b) [C<sub>2</sub>mim][OTf], (c) [C<sub>2</sub>mim][TF<sub>2</sub>N], (d) [C<sub>6</sub>mim][TF<sub>2</sub>N], (e) [C<sub>8</sub>mim][TF<sub>2</sub>N], and (f) [Amim][TF<sub>2</sub>N]. Comparisons of strategy 1 (solid lines) and strategy 2 (dashed lines) to experimental data<sup>39–42,55</sup> (symbols).

BIPs for ILs and methanol or for IL ions and methanol, as used in, respectively, strategies 1 and 2, were also set equal to 0, due to the scarcity of binary data.

For ternary systems, where data for the corresponding three binary sub-systems can be found to regress the BIPs, such as CO<sub>2</sub>/[C<sub>4</sub>mim][PF<sub>6</sub>]/water, both strategies show similar prediction accuracy, as shown in Figure 6 and the  $P - x$  phase

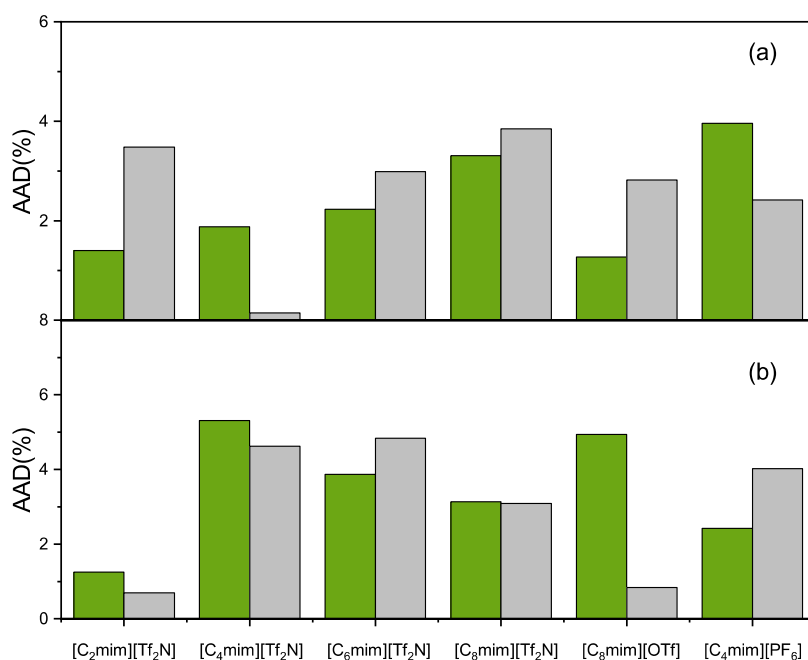


**Figure 4.** AAD (%) of mutual solubilities of (a) water in ILs and (b) ILs in water (green for strategy 1 and gray for strategy 2).

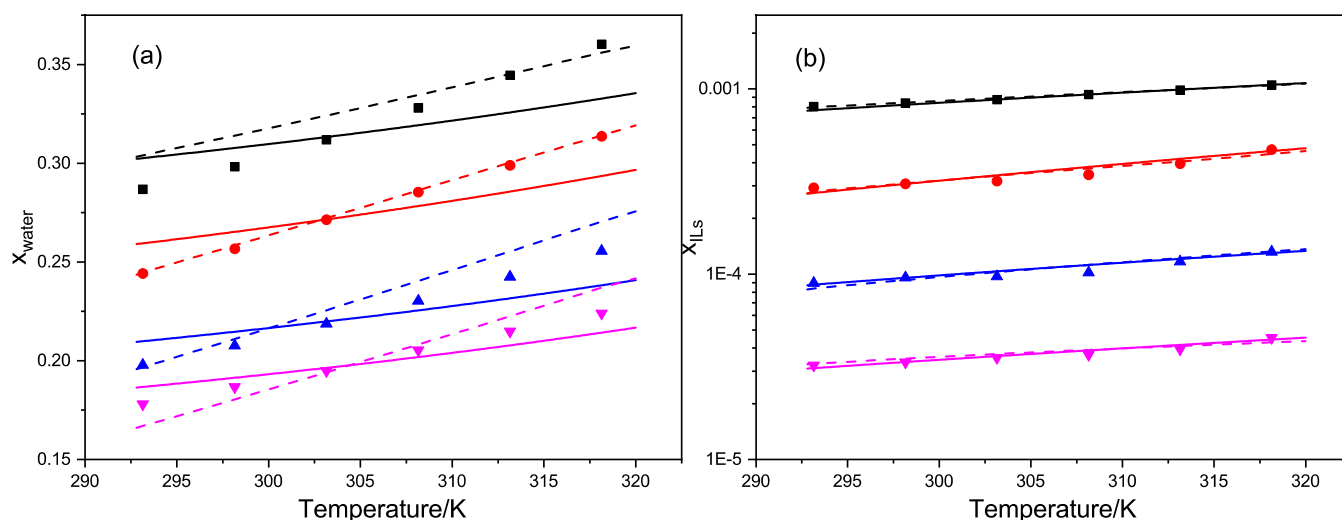


**Figure 5.** Mutual solubilities of (a) water in ILs and (b) ILs in water for  $[\text{C}_2\text{mim}][\text{TF}_2\text{N}]$  (black),  $[\text{C}_4\text{mim}][\text{TF}_2\text{N}]$  (red),  $[\text{C}_6\text{mim}][\text{TF}_2\text{N}]$  (blue), and  $[\text{C}_8\text{mim}][\text{TF}_2\text{N}]$  (magenta). Comparison of strategy 1 (solid lines) and strategy 2 (dashed lines) to experimental data<sup>56</sup> (symbols).

diagrams in Figure 7. The deviations obtained with strategy 2 are slightly larger mainly because the simplified version of the dielectric constant derivative with respect to the mole fraction, as given in eq 11, is inaccurate in the water-containing ternary systems. The solubilities of  $\text{CO}_2$  in mixtures of  $[\text{C}_4\text{mim}][\text{PF}_6]$  and water tend to decrease first and then increase with increasing water fraction, as shown in Figure 7. However, none of the two strategies can capture this trend, instead showing a monotonous decrease with increasing water fraction. The advantage of strategy 2 is that BIPs between IL ions and water can be used directly to predict phase equilibria of mixtures involving ILs composed of these IL ions. For systems of  $\text{CO}_2/[\text{C}_2\text{mim}][\text{OTf}]/\text{water}$ , the most appropriate BIPs for  $[\text{C}_2\text{mim}]^+$  and  $[\text{OTf}]^-$  with water cannot be obtained directly, because of lacking experimental data for mixtures of  $[\text{C}_2\text{mim}][\text{OTf}]$  and water. However, a set of relatively reliable BIPs can be indirectly obtained from LLE data of  $[\text{C}_2\text{mim}][\text{TF}_2\text{N}]/\text{water}$  for

$[\text{C}_2\text{mim}]^+$  and  $[\text{C}_8\text{mim}][\text{OTf}]/\text{water}$  for  $[\text{OTf}]^-$ . Figures 5 and 8 show that strategy 2 performs excellently in correlations for these two binary systems. When these BIPs were used to predict  $\text{CO}_2$  solubility in mixed solvents, better results were obtained compared to strategy 1. However, the relatively larger deviations in strategy 2 for  $\text{CO}_2/[\text{C}_2\text{mim}][\text{OTf}]/\text{water}$  than the other systems are caused by the strong correlations between BIPs for IL cations and IL anions with water in different ILs. As discussed previously, BIPs were obtained by fitting to all experimental data together, and the values of BIPs were determined by trying to balance all of the selected data. Therefore, these BIPs are often local optima for selected data, rather than global optima for all mixtures. If there are more experimental data to regress the parameters, the prediction accuracy could be significantly improved.

When it comes to methanol-containing systems, both strategies provide accurate predictions in both selected cases.

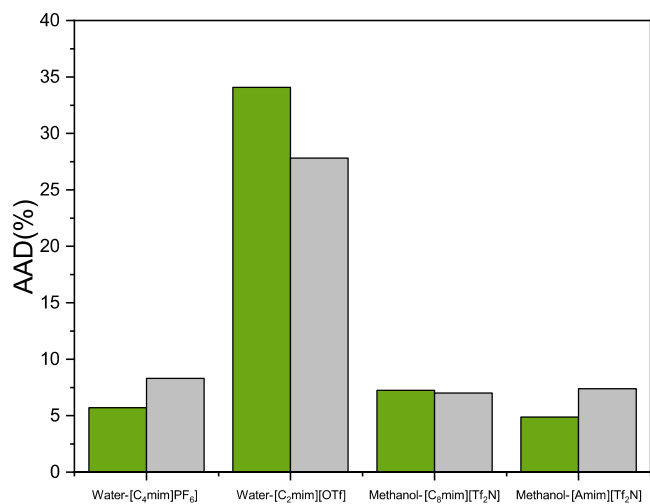


**Figure 6.** AAD (%) of CO<sub>2</sub> solubilities in mixtures of ILs and co-solvents (green for strategy 1 and gray for strategy 2).

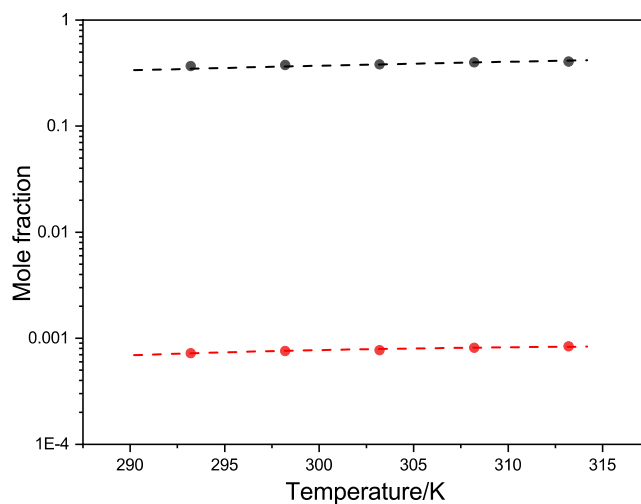


**Figure 8.** Mutual solubilities of [C<sub>8</sub>mim][OTf] and water: black for solubility of water in IL and red for solubility of IL in water. Comparison of strategy 2 (dashed lines) to experimental data<sup>58</sup> (symbols).

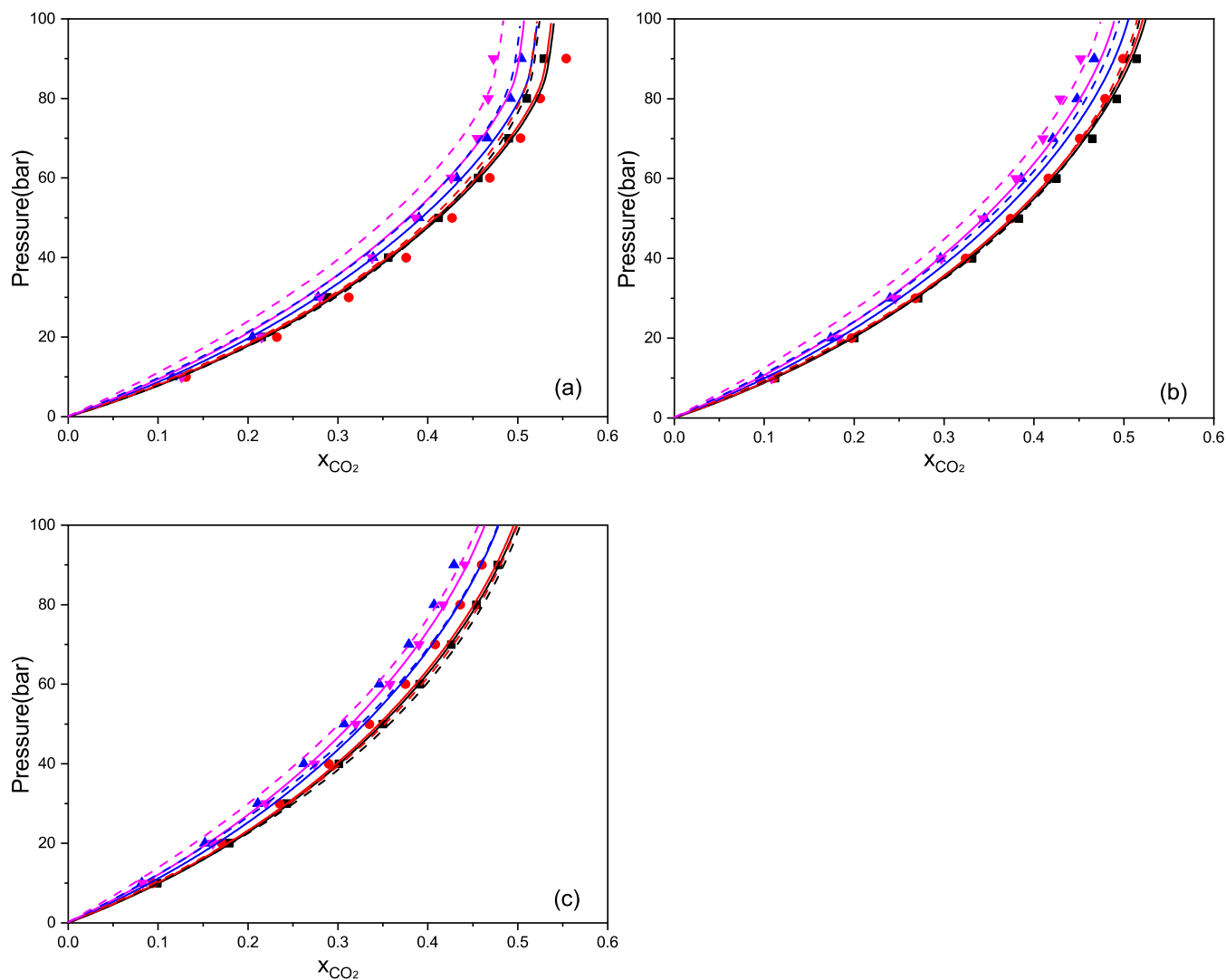


**Figure 7.** Solubilities of CO<sub>2</sub> in the binary solvent of [C<sub>4</sub>mim][PF<sub>6</sub>] and water with different mass fractions of water (black for 0%, red for 0.15%, blue for 0.89%, and magenta for 1.6%) at (a) 313.15 K, (b) 323.15 K, and (c) 333.15 K. Comparisons of strategy 1 (solid lines) and strategy 2 (dashed lines) to experimental data<sup>39</sup> (symbols).

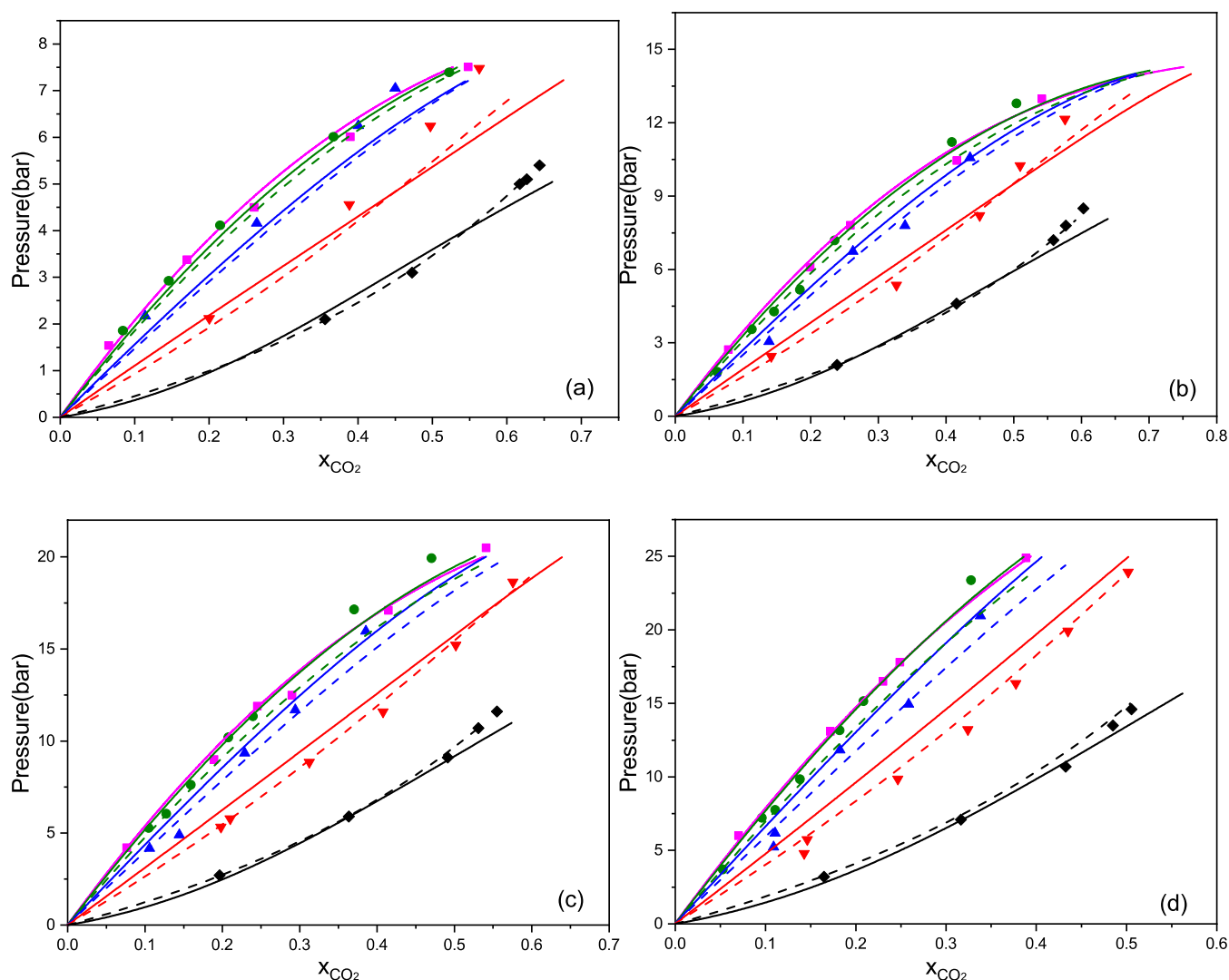


**Figure 9.** Solubilities of CO<sub>2</sub> in the binary solvent of [C<sub>8</sub>mim][Tf<sub>2</sub>N] and methanol with different mass fraction of methanol (black for 0%, red for 20%, blue for 50%, green for 80%, and magenta for 100%) at (a) 228.2 K, (b) 243.2 K, (c) 258.2 K, and (d) 273.2 K. Comparisons of strategy 1 (solid lines) and strategy 2 (dashed lines) to experimental data<sup>40</sup> (symbols).

The presence of water seriously abates the CO<sub>2</sub> solvation energy for the ILs by weakening interactions between anions and CO<sub>2</sub>.<sup>57</sup> The interactions between IL ions and methanol are not as strong as those between IL ions and water because of relatively weaker hydrogen-bonding interactions; thus, excellent predictions are obtained, even without any BIPs for IL ions and methanol. Typical predictions for CO<sub>2</sub>/[C<sub>8</sub>mim][Tf<sub>2</sub>N]/methanol are given in Figure 9. With increasing mass fraction of [C<sub>8</sub>mim][Tf<sub>2</sub>N] added to methanol, the solubility of CO<sub>2</sub> increases gradually, and the prediction lines provided by the two strategies are in good agreement with experimental data.

#### 4. CONCLUSIONS

In this work, the solubility of CO<sub>2</sub> in pure solvents, including ILs, water, and methanol, as well as binary mixtures of ILs and water or methanol was investigated. Two strategies based on PC-SAFT EoS were developed to model solubility, VLE, and LLE for these binary and ternary mixtures. In the first strategy, ILs were considered as self-associating chain molecules with two association sites. In the second strategy, they were considered to dissociate into anions and cations. BIPs used in the first strategy were obtained by fitting to the corresponding binary

experimental data, while BIPs used in the second strategy were obtained by fitting to all of the binary data together to ensure the uniformity of BIPs for different ILs composed of the same cations and anions. Ternary data were employed to verify the predictive capability.

It was found that both strategies provide accurate correlations in modeling CO<sub>2</sub> solubilities in ILs and LLE of IL/water systems. In the verification stage, both strategies can provide accurate predictions for CO<sub>2</sub> solubilities in a binary mixture of water and [C<sub>4</sub>mim][PF<sub>6</sub>]. However, larger deviations were obtained for a ternary mixture of CO<sub>2</sub>/[C<sub>2</sub>mim][OTf]/water due to the scarcity of experimental data to regress the BIPs for ILs or IL ions with water. The second strategy performs better than the first one because BIPs for IL ions with water can be obtained by fitting to data of other ILs composed of the same cations and anions, which is an advantage. For cases of CO<sub>2</sub>/ILs/methanol, accurate predictions were obtained with both strategies, even without any BIPs used to correct interactions between ILs or IL ions and methanol. More experimental data for binary mixtures of ILs and co-solvents are necessary for PC-SAFT EoS to serve as an ideal tool for phase equilibria



calculations in CO<sub>2</sub> capturing processes with IL-based solvents as absorbents.

## ■ ASSOCIATED CONTENT

### SI Supporting Information

The Supporting Information is available free of charge at <https://pubs.acs.org/doi/10.1021/acs.iecr.2c02778>.

Deviations and binary interaction parameters for CO<sub>2</sub> solubilities in water and methanol; CO<sub>2</sub> solubilities in ILs; mutual solubilities of ILs and water; and prediction results for ternary systems (PDF)

## ■ AUTHOR INFORMATION

### Corresponding Authors

**Ke Zheng** – Beijing Key Laboratory of Coal to Cleaning Liquid Fuels, National Energy R & D Center for Coal to Liquid Fuels, Synfuels China Co., Ltd., Beijing 101400, P. R. China; Centre for Nature-Inspired Engineering, Department of Chemical Engineering, University College London (UCL), London WC1E 7JE, U.K.; [orcid.org/0000-0001-7429-6420](https://orcid.org/0000-0001-7429-6420); Email: [zhengke13@mails.ucl.ac.uk](mailto:zhengke13@mails.ucl.ac.uk)

**Marc-Olivier Coppens** – Centre for Nature-Inspired Engineering, Department of Chemical Engineering, University College London (UCL), London WC1E 7JE, U.K.; [orcid.org/0000-0002-1810-2537](https://orcid.org/0000-0002-1810-2537); Email: [m.coppens@ucl.ac.uk](mailto:m.coppens@ucl.ac.uk)

### Authors

**Xinyu Liao** – Centre for Nature-Inspired Engineering, Department of Chemical Engineering, University College London (UCL), London WC1E 7JE, U.K.

**Gang Wang** – Beijing Key Laboratory of Coal to Cleaning Liquid Fuels, National Energy R & D Center for Coal to Liquid Fuels, Synfuels China Co., Ltd., Beijing 101400, P. R. China; [orcid.org/0000-0003-1222-2893](https://orcid.org/0000-0003-1222-2893)

**Yong Yang** – Beijing Key Laboratory of Coal to Cleaning Liquid Fuels, National Energy R & D Center for Coal to Liquid Fuels, Synfuels China Co., Ltd., Beijing 101400, P. R. China; [orcid.org/0000-0002-9220-6166](https://orcid.org/0000-0002-9220-6166)

**Yongwang Li** – Beijing Key Laboratory of Coal to Cleaning Liquid Fuels, National Energy R & D Center for Coal to Liquid Fuels, Synfuels China Co., Ltd., Beijing 101400, P. R. China

Complete contact information is available at: <https://pubs.acs.org/doi/10.1021/acs.iecr.2c02778>

### Notes

The authors declare no competing financial interest.

## ■ ACKNOWLEDGMENTS

K.Z. gratefully acknowledges the Strategic Priority Research Program of the Chinese Academy of Sciences (Grant No. XDA21020100) for financial support. Marc-Olivier Coppens is grateful to Synfuels China for supporting K.Z.'s stay at UCL.

## ■ REFERENCES

- (1) Oh, T. H. Carbon capture and storage potential in coal-fired plant in Malaysia—A review. *Renewable Sustainable Energy Rev.* **2010**, *14*, 2697–2709.
- (2) Benson, S. M.; Orr, F. M. Carbon Dioxide Capture and Storage. *MRS Bull.* **2008**, *33*, 303–305.
- (3) Olajire, A. A. CO<sub>2</sub> capture and separation technologies for end-of-pipe applications – A review. *Energy* **2010**, *35*, 2610–2628.
- (4) Mirzaei, S.; Shamiri, A.; Aroua, M. K. A review of different solvents, mass transfer, and hydrodynamics for postcombustion CO<sub>2</sub> capture. *Rev. Chem. Eng.* **2015**, *31*, 521–561.
- (5) Yu, C.-H.; Huang, C.-H.; Tan, C.-S. A Review of CO<sub>2</sub> Capture by Absorption and Adsorption. *Aerosol. Air. Qual. Res.* **2012**, *12*, 745–769.
- (6) Desideri, U. Advanced Absorption Processes and Technology for Carbon Dioxide (CO<sub>2</sub>) Capture in Power Plants. In *Developments and Innovation in Carbon Dioxide (CO<sub>2</sub>) Capture and Storage Technology*, Maroto-Valer, M. M., Ed.; Woodhead Publishing Series in Energy, 2010; Vol. 1, pp 155–182.
- (7) Kohl, A. L.; Nielsen, R. B. Physical Solvents for Acid Gas Removal. In *Gas Purification*, 5th ed.; Kohl, A. L.; Nielsen, R. B., Eds.; Gulf Professional Publishing: Houston, 1997; pp 1187–1237.
- (8) Kidnay, A. J.; Parrish, W. R.; McCartney, D. G. *Fundamentals of Natural Gas Processing*, 3rd ed.; CRC Press: Boca Raton, 2019.
- (9) Tan, Y.; Nookuea, W.; Li, H.; Thorin, E.; Yan, J. Property impacts on Carbon Capture and Storage (CCS) processes: A review. *Energy Convers. Manage.* **2016**, *118*, 204–222.
- (10) Sun, L.; Smith, R. Rectisol wash process simulation and analysis. *J. Clean. Prod.* **2013**, *39*, 321–328.
- (11) Ramdin, M.; de Loos, T. W.; Vlugt, T. J. H. State-of-the-Art of CO<sub>2</sub> Capture with Ionic Liquids. *Ind. Eng. Chem. Res.* **2012**, *51*, 8149–8177.
- (12) Babamohammadi, S.; Shamiri, A.; Aroua, M. K. A review of CO<sub>2</sub> capture by absorption in ionic liquid-based solvents. *Rev. Chem. Eng.* **2015**, *31*, 383–412.
- (13) Aghaie, M.; Rezaei, N.; Zendeheboudi, S. A systematic review on CO<sub>2</sub> capture with ionic liquids: Current status and future prospects. *Renewable Sustainable Energy Rev.* **2018**, *96*, 502–525.
- (14) Zhang, X.; Zhang, X.; Dong, H.; Zhao, Z.; Zhang, S.; Huang, Y. Carbon capture with ionic liquids: overview and progress. *Energy Environ. Sci.* **2012**, *5*, 6668–6681.
- (15) Karadas, F.; Atilhan, M.; Aparicio, S. Review on the Use of Ionic Liquids (ILs) as Alternative Fluids for CO<sub>2</sub> Capture and Natural Gas Sweetening. *Energy Fuels* **2010**, *24*, 5817–5828.
- (16) Tang, J.; Sun, W.; Tang, H.; Radosz, M.; Shen, Y. Enhanced CO<sub>2</sub> Absorption of Poly(ionic liquid)s. *Macromolecules* **2005**, *38*, 2037–2039.
- (17) Zhou, Q.; Wang, L.-S.; Chen, H.-P. Densities and Viscosities of 1-Butyl-3-methylimidazolium Tetrafluoroborate + H<sub>2</sub>O Binary Mixtures from (303.15 to 353.15) K. *J. Chem. Eng. Data* **2006**, *51*, 905–908.
- (18) Carvalho, P. J.; Regueira, T.; Santos, L. M. N. B. F.; Fernandez, J.; Coutinho, J. A. P. Effect of Water on the Viscosities and Densities of 1-Butyl-3-methylimidazolium Dicyanamide and 1-Butyl-3-methylimidazolium Tricyanomethane at Atmospheric Pressure. *J. Chem. Eng. Data* **2010**, *55*, 645–652.
- (19) Husson, P.; Pison, L.; Jacquemin, J.; Gomes, M. F. C. Influence of water on the carbon dioxide absorption by 1-ethyl-3-methylimidazolium bis(trifluoromethylsulfonyl)amide. *Fluid Phase Equilib.* **2010**, *294*, 98–104.
- (20) Fendt, S.; Padmanabhan, S.; Blanch, H. W.; Prausnitz, J. M. Viscosities of Acetate or Chloride-Based Ionic Liquids and Some of Their Mixtures with Water or Other Common Solvents. *J. Chem. Eng. Data* **2011**, *56*, 31–34.
- (21) Tian, S.; Hou, Y.; Wu, W.; Ren, S.; Pang, K. Physical Properties of 1-Butyl-3-methylimidazolium Tetrafluoroborate/N-Methyl-2-pyrrolidone Mixtures and the Solubility of CO<sub>2</sub> in the System at Elevated Pressures. *J. Chem. Eng. Data* **2012**, *57*, 756–763.
- (22) Ma, C.; Laaksonen, A.; Liu, C.; Lu, X.; Ji, X. The peculiar effect of water on ionic liquids and deep eutectic solvents. *Chem. Soc. Rev.* **2018**, *47*, 8685–8720.
- (23) Ji, X.; Held, C.; Sadowski, G. Modeling imidazolium-based ionic liquids with ePC-SAFT. *Fluid Phase Equilib.* **2012**, *335*, 64–73.
- (24) Polishuk, I. Implementation of CP-PC-SAFT for Predicting Thermodynamic Properties and Gas Solubility in 1-Alkyl-3-methylimidazolium Bis(trifluoromethylsulfonyl)imide Ionic Liquids without Fitting Binary Parameters. *Ind. Eng. Chem. Res.* **2017**, *56*, 7845–7857.
- (25) Polishuk, I. Wide-ranging prediction of phase behavior in complex systems by CP-PC-SAFT with universal kij values. I. Mixtures

- of non-associating compounds with [C2mim][EtSO<sub>4</sub>], [C4mim]-[MeSO<sub>4</sub>], and [C2mim][MeSO<sub>3</sub>] ionic liquids. *J. Mol. Liq.* **2020**, *310*, No. 113266.
- (26) Bülow, M.; Gerek Ince, N.; Hirohama, S.; Sadowski, G.; Held, C. Predicting Vapor–Liquid Equilibria for Sour-Gas Absorption in Aqueous Mixtures of Chemical and Physical Solvents or Ionic Liquids with ePC-SAFT. *Ind. Eng. Chem. Res.* **2021**, *60*, 6327–6336.
- (27) Pabsch, D.; Held, C.; Sadowski, G. Modeling the CO<sub>2</sub> Solubility in Aqueous Electrolyte Solutions Using ePC-SAFT. *J. Chem. Eng. Data* **2020**, *65*, 5768–5777.
- (28) Ji, X.; Held, C.; Sadowski, G. Modeling imidazolium-based ionic liquids with ePC-SAFT. Part II. Application to H<sub>2</sub>S and synthesis-gas components. *Fluid Phase Equilib.* **2014**, *363*, 59–65.
- (29) Llovel, F.; Vega, L. F. Assessing Ionic Liquids Experimental Data Using Molecular Modeling: [Cnmim][BF<sub>4</sub>] Case Study. *J. Chem. Eng. Data* **2014**, *59*, 3220–3231.
- (30) Jalili, A. H.; Safavi, M.; Ghotbi, C.; Mehdizadeh, A.; Hosseini-Jenab, M.; Taghikhani, V. Solubility of CO<sub>2</sub>, H<sub>2</sub>S, and Their Mixture in the Ionic Liquid 1-Octyl-3-methylimidazolium Bis(trifluoromethyl)sulfonylimide. *J. Phys. Chem. B.* **2012**, *116*, 2758–2774.
- (31) Wertheim, M. S. Fluids with highly directional attractive forces. 1. statistical thermodynamics. *J. Stat. Phys.* **1984**, *35*, 19–34.
- (32) Wertheim, M. S. Fluids with highly directional attractive forces. 2. thermodynamic perturbation-theory and integral-equations. *J. Stat. Phys.* **1984**, *35*, 35–47.
- (33) Wertheim, M. S. Fluids with highly directional attractive forces. 3. multiple attraction sites. *J. Stat. Phys.* **1986**, *42*, 459–476.
- (34) Wertheim, M. S. Fluids with highly directional attractive forces. 4. equilibrium polymerization. *J. Stat. Phys.* **1986**, *42*, 477–492.
- (35) Baramaki, Z.; Arab Aboosadi, Z.; Esfandiari, N. Fluid phase equilibrium prediction of acid gas solubility in imidazolium-based ionic liquids with the Peng-Robinson and the PC-SAFT models. *Pet. Sci. Technol.* **2019**, *37*, 110–117.
- (36) Al-fnaish, H.; Lue, L. Modelling the solubility of H<sub>2</sub>S and CO<sub>2</sub> in ionic liquids using PC-SAFT equation of state. *Fluid Phase Equilib.* **2017**, *450*, 30–41.
- (37) Bülow, M.; Ji, X.; Held, C. Incorporating a concentration-dependent dielectric constant into ePC-SAFT. An application to binary mixtures containing ionic liquids. *Fluid Phase Equilib.* **2019**, *492*, 26–33.
- (38) Liu, Z.; Wu, W.; Han, B.; Dong, Z.; Zhao, G.; Wang, J.; Jiang, T.; Yang, G. Study on the Phase Behaviors, Viscosities, and Thermodynamic Properties of CO<sub>2</sub>/[C4mim][PF<sub>6</sub>]/Methanol System at Elevated Pressures. *Chem. - Eur. J.* **2003**, *9*, 3897–3903.
- (39) Fu, D.; Sun, X.; Pu, J.; Zhao, S. Effect of Water Content on the Solubility of CO<sub>2</sub> in the Ionic Liquid [bmim][PF<sub>6</sub>]. *J. Chem. Eng. Data* **2006**, *51*, 371–375.
- (40) Dai, C.; Wei, W.; Lei, Z.; Li, C.; Chen, B. Absorption of CO<sub>2</sub> with methanol and ionic liquid mixture at low temperatures. *Fluid Phase Equilib.* **2015**, *391*, 9–17.
- (41) Taheri, M.; Dai, C.; Lei, Z. CO<sub>2</sub> capture by methanol, ionic liquid, and their binary mixtures: Experiments, modeling, and process simulation. *AIChE J.* **2018**, *64*, 2168–2180.
- (42) Zakrzewska, M. E.; Nunes da Ponte, M. Influence of Water on the Carbon Dioxide Solubility in [OTf]- and [eFAP]-Based Ionic Liquids. *J. Chem. Eng. Data* **2018**, *63*, 907–912.
- (43) Aghaie, M.; Rezaei, N.; Zendejboudi, S. Assessment of carbon dioxide solubility in ionic liquid/toluene/water systems by extended PR and PC-SAFT EOSs: Carbon capture implication. *J. Mol. Liq.* **2019**, *275*, 323–337.
- (44) Ma, C.; Shukla, S. K.; Samikannu, R.; Mikkola, J.-P.; Ji, X. CO<sub>2</sub> Separation by a Series of Aqueous Morpholinium-Based Ionic Liquids with Acetate Anions. *ACS Sustainable Chem. Eng.* **2020**, *8*, 415–426.
- (45) Gross, J.; Sadowski, G. Perturbed-Chain SAFT: An Equation of State Based on a Perturbation Theory for Chain Molecules. *Ind. Eng. Chem. Res.* **2001**, *40*, 1244–1260.
- (46) Gross, J.; Sadowski, G. Application of the Perturbed-Chain SAFT Equation of State to Associating Systems. *Ind. Eng. Chem. Res.* **2002**, *41*, 5510–5515.
- (47) Cameretti, L. F.; Sadowski, G.; Mollerup, J. M. Modeling of Aqueous Electrolyte Solutions with Perturbed-Chain Statistical Associated Fluid Theory. *Ind. Eng. Chem. Res.* **2005**, *44*, 3355–3362.
- (48) Held, C.; Reschke, T.; Mohammad, S.; Luza, A.; Sadowski, G. ePC-SAFT revised. *Chem. Eng. Res. Des.* **2014**, *92*, 2884–2897.
- (49) Zheng, K.; Wu, H.; Geng, C.; Wang, G.; Yang, Y.; Li, Y. A Comparative Study of the Perturbed-Chain Statistical Associating Fluid Theory Equation of State and Activity Coefficient Models in Phase Equilibria Calculations for Mixtures Containing Associating and Polar Components. *Ind. Eng. Chem. Res.* **2018**, *57*, 3014–3030.
- (50) Zheng, K.; Yang, R.; Wu, H.; Wang, G.; Yang, Y.; Li, Y. Application of the Perturbed-Chain SAFT to Phase Equilibria in the Fischer–Tropsch Synthesis. *Ind. Eng. Chem. Res.* **2019**, *58*, 8387–8400.
- (51) Nonthanasin, T.; Henni, A.; Saiwan, C. Densities and low pressure solubilities of carbon dioxide in five promising ionic liquids. *RSC Adv.* **2014**, *4*, 7566–7578.
- (52) Fernández, D. P.; Goodwin, A. R. H.; Lemmon, E. W.; Sengers, J. M. H. L.; Williams, R. C. A Formulation for the Static Permittivity of Water and Steam at Temperatures from 238 K to 873 K at Pressures up to 1200 MPa, Including Derivatives and Debye–Hückel Coefficients. *J. Phys. Chem. Ref. Data* **1997**, *26*, 1125–1166.
- (53) Held, C.; Prinz, A.; Wallmeyer, V.; Sadowski, G. Measuring and modeling alcohol/salt systems. *Chem. Eng. Sci.* **2012**, *68*, 328–339.
- (54) Bamberger, A.; Sieder, G.; Maurer, G. High-pressure (vapor+liquid) equilibrium in binary mixtures of (carbon dioxide+water or acetic acid) at temperatures from 313 to 353 K. *J. Supercrit. Fluids* **2000**, *17*, 97–110.
- (55) Carvalho, P. J.; Álvarez, V. H.; Marrucho, I. M.; Aznar, M.; Coutinho, J. A. P. High pressure phase behavior of carbon dioxide in 1-butyl-3-methylimidazolium bis(trifluoromethylsulfonyl)imide and 1-butyl-3-methylimidazolium dicyanamide ionic liquids. *J. Supercrit. Fluids* **2009**, *50*, 105–111.
- (56) Freire, M. G.; Carvalho, P. J.; Gardas, R. L.; Marrucho, I. M.; Santos, L. M. N. B. F.; Coutinho, J. A. P. Mutual Solubilities of Water and the [Cnmim][Tf<sub>2</sub>N] Hydrophobic Ionic Liquids. *J. Phys. Chem. B* **2008**, *112*, 1604–1610.
- (57) Yang, F.; Wang, X.; Liu, Y.; Yang, Y.; Zhao, M.; Liu, X.; Li, W. Understanding CO<sub>2</sub> capture kinetics and energetics by ionic liquids with molecular dynamics simulation. *RSC Adv.* **2020**, *10*, 13968–13974.
- (58) Santos, D.; Góes, M.; Franceschi, E.; Santos, A.; Dariva, C.; Fortuny, M.; Mattedi, S. Phase equilibria for binary systems containing ionic liquid with water or hydrocarbons. *Braz. J. Chem. Eng.* **2015**, *32*, 967–974.